A ES
ISSN: 2096-3246
Volume 58, Issue 01, 2026

EFFECT OF TOOL ROTATIONAL SPEED ON MICROSTRUCTURE AND MECHANICAL PROPERTIES OF FRICTION STIR WELDING OF AA6351-T6 ALUMINIUM ALLOY TO INTERSTITIAL-FREE STEEL

Mukesh Kumar [1*] , Amar Nath Sinha[2]
Mechanical Engineering Department, NIT Patna-800005, India.
Faculty of Mechanical Engineering Department, NIT Patna-800005, India.
*Corresponding Author's Email: mukeshk.phd19.me@nitp.ac.in

ABSTRACT
This study investigates the influence of tool rotational speed on microstructure and mechanical properties of friction stir welded joints between AA6351-T6 aluminium alloy and interstitial-free steel. The welds were produced at rotational speeds ranging from 200 to 1000 rpm at the processing interval of 200rpm for a constant traverse speed of 55 mm/min. Microstructural examination revealed Fe_3Al and Fe_2Al_5 intermetallic compounds at the Al/Fe interface, with thickness varying from 0.87 to 2.09 μm depending on rotational speed. Optimal joint strength of 184.42 MPa, approximately 75% of base aluminium alloy was achieved at 600 rpm, representing an ideal balance between effective material mixing and controlled intermetallic layer formation. Higher rotational speeds produced excessive heat input and thicker intermetallic layers, deteriorating joint strength. Fractography showed a transition from ductile to mixed-mode fracture with increasing rotational speed.

KEYWORDS: "Aluminium alloy, Friction stir welding, Intermetallic compounds, Interstitial-free steel"

1. INTRODUCTION
The demand for multi-material structures that combine the advantages of different materials has substantially increased in recent years, particularly in the automotive, aerospace, and shipbuilding industries [1-3]. Lightweight structures that incorporate both aluminium alloys and steel are especially attractive, as they offer improved fuel efficiency through weight reduction while maintaining structural integrity and crash resistance [4, 5]. Among the various aluminium alloys, the 6xxx series alloys, particularly AA6351-T6, are widely preferred for their excellent combination of strength, formability, and corrosion resistance [6].

In conventional fusion welding of aluminium to steel, the primary challenges include: Significant differences in physical and metallurgical properties [7], formation of thick, brittle Fe-Al intermetallic compounds at the weld region[8], substantial differences in thermal expansion coefficients, resulting in high residual stresses and distortion [9]; and creation of porosity and hot cracking due to hydrogen solubility[10].Friction stir welding (FSW) has emerged as a promising alternative for joining dissimilar materials [11]. The frictional heat generated between the tool and workpieces, combined with severe plastic deformation, leads to material softening and mixing without reaching the melting point [12, 13]. FSW of aluminium to steel remains challenging due to the significant differences in mechanical properties and flow stresses between these materials,

as well as the inevitable formation of intermetallic compounds, albeit to a lesser extent than in fusion welding [14, 15].

Liu et al. [16] provided a comprehensive review on the progress in dissimilar friction stir welding of aluminium alloy and steel. Tool rotational speed is considered one of the most influential parameters in FSW, as it directly affects heat generation, material flow, and consequently, the microstructural evolution and mechanical properties of the joints [17,18]. Recent investigations by Wang et al. [19] on the effect of tool pin diameter and Shen et al. [20] on direct bonding mechanisms have further advanced our understanding of the process. However, a systematic study on the effect of tool rotational speed on microstructure and mechanical properties of FSW joints between AA6351-T6 aluminium alloy and IF steel is still lacking in the literature. So, the present studies intend to investigate the effect of tool rotational speed on the microstructure and mechanical properties of the joints.

2. MATERIAL AND METHODS

The Friction Stir Welding of base materials used in this study were AA6351-T6 aluminium alloy and Interstitial Free (IF) steel with dimensions of 140 mm × 70 mm × 3 mm. The chemical compositions and the mechanical properties of both materials are presented in Table 1 and Table 2 respectively.

Table.1. Chemical compositions of IF steel and Al 6351-T6 (wt %)

Metals	C	Mn	Mg	Si	S	P	Ti	Bal.
IF Steel	0.0019	0.62		0.011	0.007	0.011	0.064	Fe
Al6351	-	0.6	0.6	1.1	-	-	-	Al

Table 2 Mechanical properties IF steel and Al 6351-T6

Alloys	Yield strength (MPa)	Ultimate tensile strength (MPa)	Elongation (%)
IF steel	132.2±2.5	267.2±3.2	34 ±4.2
Al6351-T6	122±3.2	250.2 ±2.8	15.5±1.8

Friction stir welding was performed by using FSW tool made up of a tungsten carbide (WC) pin and high-speed steel shoulder. The tool dimensions and FSW processing) images are illustrated in Figure 1(a) & 1(b) respectively. Welding experiments were conducted at varying tool rotational speeds (200, 400, 600, 800, and 1000 rpm) at a constant traverse speed of 55 mm/min and a tool tilt angle of 2°. The IF steel and AA6351-T6 plates were positioned at the advancing and retreating sides, respectively, and rigidly clamped to prevent displacement during welding.

ISSN: 2096-3246
Volume 58, Issue 01, 2026

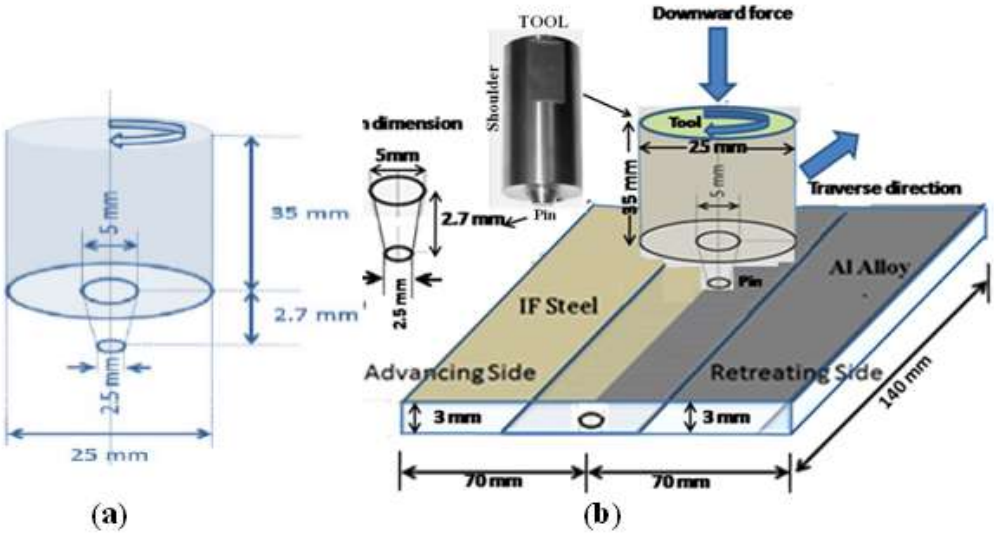

Figure 1. Schematic diagram of (a) tool dimension and (b) FSW processing diagram.

2.1 Heat Input Calculation

The frictional heat generated during welding was calculated using Frigaard's equation [21]:

$$Q_0 = \frac{4}{3}\pi r^2 \mu P \omega R^3 \quad (1)$$

Where Q_0 represents heat input (net power), μ is the friction coefficient, P denotes the applied pressure, ω is the tool rotational speed (rad/s), and R is the tool shoulder radius.

2.2 Characterization Techniques

Transverse sections were cut from the welded assemblies for metallographic examination. Samples were prepared following standard metallographic procedures and etched with Keller's reagent for aluminium and 2% Nital for steel. Microstructural characterization was performed using optical microscopy and scanning electron microscopy (Carl Zeiss-Supra 25 FEG) equipped with energy-dispersive X-ray spectroscopy (Oxford Instrument INCA Penta FETX3).The grain size at the stir zone (SZ) was measured by line intercept method of the optical images. Phase identification at the weld interface was conducted using X-ray diffraction (Philips Panalytical Xpertpro) with Cu Kα radiation (λ = 1.5406 Å) at a step size of 0.001° over a 2θ range of 20-90°. Tensile testing was performed according to ASTM E8/E8M-11 standards using an Instron 5582 universal testing machine at a crosshead speed of 0.5 mm/min. Fractographic examination of tensile specimens was conducted using same scanning electron microscopy to analyze the failure mechanisms.

3. Results and Discussion

3.1 Macrostructure and Surface Appearance

Figure 2 shows the surface appearance of the friction stir welded joints produced at different rotational speeds. At 200 rpm (Figure 2a), the weld surface exhibited significant surface line defects shown by arrow mark, indicating insufficient heat input and poor material flow. As the rotational speed increased to 400 rpm to 800 rpm (Figure 2 b-2d), the surface quality improved considerably, without any defects. However at 1000 rpm (Figure 2e) groove defects (marked by arrow) was detected due to increased heat input and material softening.

ISSN: 2096-3246
Volume 58, Issue 01, 2026

Figure 2 Surface appearance of FSWed joints at variable tool rotational speeds.

3.2 Microstructural Analysis

3.2.1 Weld Zone microstructure

The cross-sectional optical microstructures of the welded joints shown in Figure 3 and 4 revealed distinct weld regions, material flow patterns; from large steel particles to equiaxed recrystallised Fe-Al grains with formation of different intermetallics reaction layers in the weld regions and at the interface due to the variable rotational speed. At 200 rpm (Figure 3a) and 400 rpm (Figure 3b), the joints exhibited defragmented large number of iron particles all around in the SZ. At both tool rotational speeds smooth onion rings were observed. The joint produced at 600 rpm (Figure 3c and 3d) showed optimal material mixing with no detectable defects and scattered minute steel fragments in the aluminium side, indicating a well-consolidated weld with equiaxed Fe-Al particles at SZ. Figure 4 for rotational speeds of 800 rpm (Figure 4a & 4b) and 1000 rpm (Figure 4c & 4d) showed excessive material stirring. The joint produced at 1000 rpm showed equiaxed recrystallised Fe-Al grains with no visible defects with the formation of vortex-like along with onion type flow patterns were evident at the SZ. The IF steel side exhibited elongated grains at TMAZ while coarser grains at the HAZ region were clearly visible. Notably, the TMAZ and HAZ zones were distinctly clear and well-defined on the steel side as compared to the

ISSN: 2096-3246
Volume 58, Issue 01, 2026

aluminum side. These findings align with the observations of Kumar and Wu [22] for dissimilar Al-Fe FSW joints.

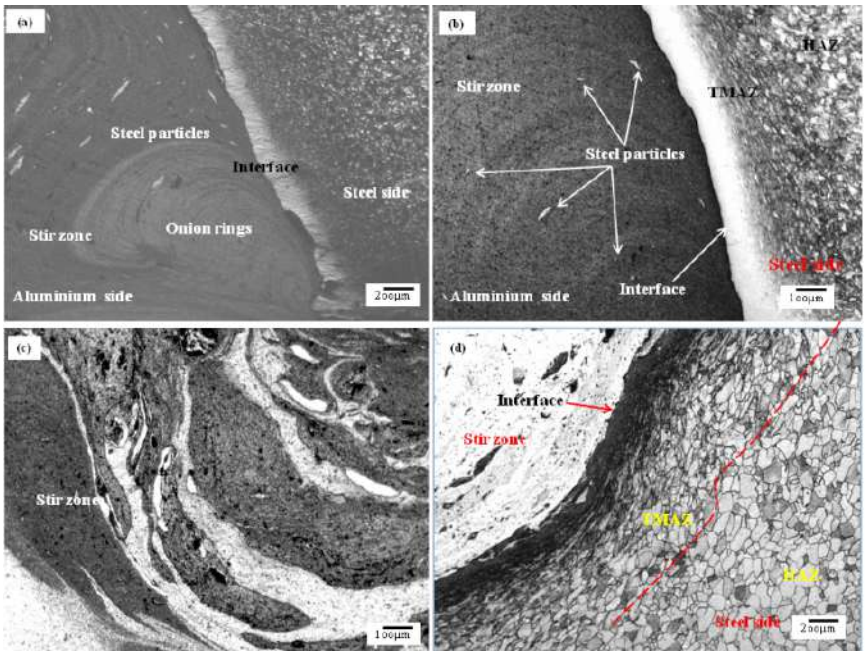

Figure 3 Optical microstructure of friction stir welded joint at (a) 200 rpm, (b) 400 rpm, (c) 600 rpm, Al-side and (d) 600 rpm, steel side.

At 200 rpm (Figure 3a), the average grain size of the steel particles in the stir zone was approximately 8.7 μm, which further decreased to 5.3 μm, 4.1 μm, 3.5 μm, and 3.2 μm at 400 rpm (Figure 3b), 600 rpm (Figure 3c & 3d), 800 rpm (Figure 4a & 4b), and 1000 rpm (Figure 4c & 4d), respectively. The aluminium in the SZ showed partially recrystallized grains with a non-uniform size distribution, indicating incomplete dynamic recrystallization due to insufficient strain and thermal energy. As the rotational speed increased the grain structure became more uniform and equiaxed, with average grain sizes of 8.5 μm and 6.2 μm, respectively. This refinement is attributed to the increased strain rate and peak temperature, promoting complete dynamic recrystallization. In the stir zone, significant grain refinement was observed at all rotational speeds. The contrasting grain size trends in the aluminium and steel stir zones can be attributed to the different recrystallization behaviors of these materials.

ISSN: 2096-3246
Volume 58, Issue 01, 2026

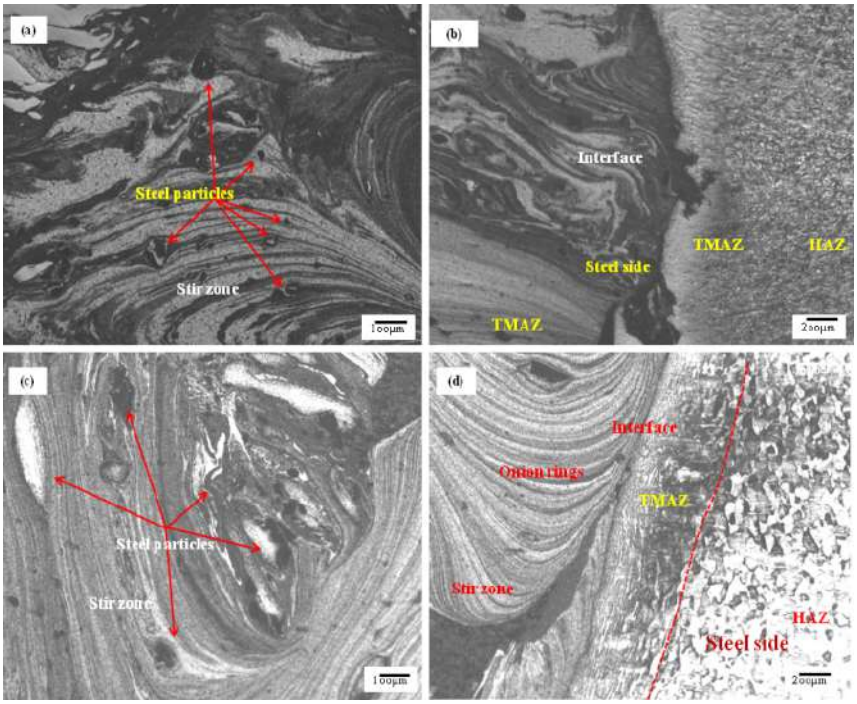

Figure 4 Optical microstructure of FSWed joint at (a) 800 rpm, (b) 800 rpm, (c) 1000 rpm, at Al alloy side; (d) 1000 rpm, at the steel side

3.2.2 Intermetallic Compound Formation

Figure 5 shows the SEM micrographs of the Al-Fe interface at different rotational speeds, revealing the presence of a continuous intermetallic layer. The thickness of this layer varied significantly with rotational speed, as summarized in Table 3.At 200 rpm (Figure 5a), a thin, discontinuous intermetallic layer with an average thickness of 0.87 μm was observed, indicating limited diffusion due to low heat input. As the rotational speed increased to 400 rpm (Figure 5b) and 600 rpm (Figure 5c), the intermetallic layer became more continuous and uniform, with thicknesses of 1.25 μm and 1.58 μm, respectively. At higher rotational speeds of 800 rpm (Figure 5d) and 1000 rpm (Figure 5e), the intermetallic layer thickness increased to 1.82 μm and 2.09 μm, respectively.

Table 3 Width of IMCs layer, Heat Input and Joint strength

Tool rotational speed (rpm)	Width of IMCs layer (μm)	Heat input (J/S)	Joint strength (MPa)
200	0.87	10.66	139.69
400	0.97	21.85	176.29
600	1.01	30.46	181.42
800	1.10	37.42	177.18
1000	2.09	54.63	106.39

ISSN: 2096-3246
Volume 58, Issue 01, 2026

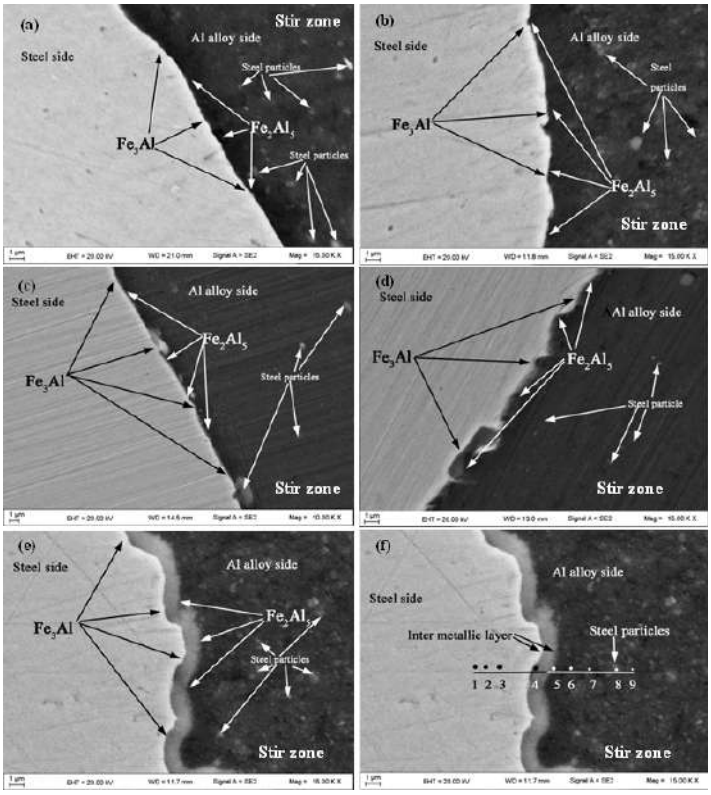

Figure 5 SEM-BSE image at interface region for the tool rpm (a) 200, (b) 400, (c) 600, (d) 800,(e) 1000 and (f) EDS analysis of line profile at 1000 rpm

EDS line scanning across the interface from aluminium to steel side (Figure 5f) revealed gradual compositional changes indicating the formation of only two intermetallic phases i.e. Fe2Al5 and Fe3Al increase of weight percentage of Fe from 0.08,0.96,3.59, 24.46,74.41, 89.48, 91.43, 87.13, and 90.81(Point no. 1-9) ,however with decreased percentage of aluminium from 91.71, 90.78,87.67,70.12,23.07,8.79,6.79, and 7.6.

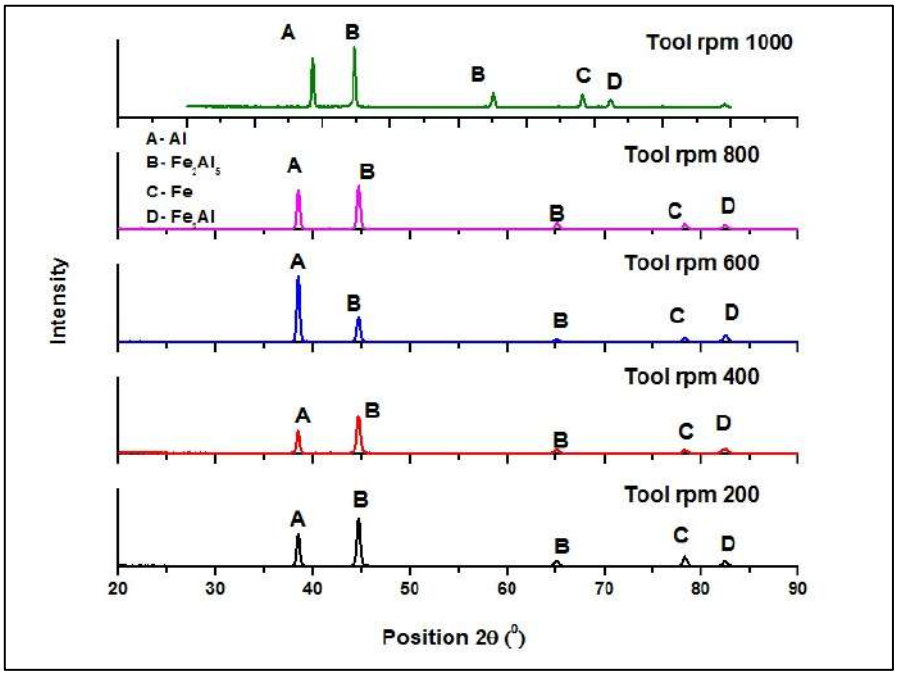

Figure 6 XRD analysis of joints at tool rpm (a)200, (b)400, (c),600, (d)800, and (e)1000

The formation and growth of intermetallic compounds in FSW of aluminium to steel follow a complex mechanism, as discussed by Kasai et al. [23] and Eslami et al. [24]. Initially, diffusion of aluminium atoms into steel occurs at the interface, leading to the formation of a thin Fe-rich Fe_3Al layer. As the process continues, additional aluminium diffuses through this layer, resulting in the formation of an Al-rich Fe_2Al_5 layer. The growth rate of these intermetallic layers is strongly temperature-dependent. Khodaverdizadeh et al. [25], who reported a similar trend in FSW of AA6061-T6 to AISI 304 stainless steel. This behavior can be attributed to the increased peak temperature and thermal cycle duration at higher rotational speeds, promoting enhanced diffusion and reaction between aluminium and iron.

3.3 Mechanical Properties

3.3.1 Tensile Properties

The effect of rotational speed and the Correlation among tool rotation speed, width of intermetallic layer, heat input and tensile properties of the FSW joints is illustrated in Figure 7 and summarized in Table 4. The joint produced at 200 rpm exhibited the lowest tensile strength of 112.34 MPa, corresponding to a joint efficiency of 45.85%. This poor performance can be attributed to insufficient heat input, resulting in incomplete bonding and inadequate material mixing. As the rotational speed increased to 400 rpm, the tensile strength improved to 156.73 MPa (joint efficiency of 63.97%) due to enhanced material flow and better consolidation.

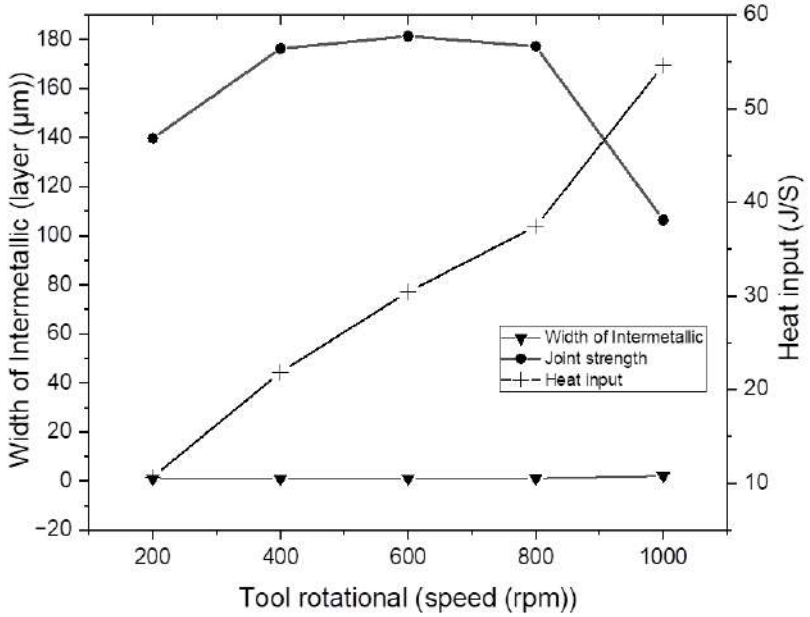

Figure 7 Correlation among tool rotation speed, width of IMCs layer, heat input and UTS of joints.

Table 4 Tensile properties of FSW joints at different rotational speeds

Rotational Speed (rpm)	Ultimate Tensile Strength (MPa)	Joint Efficiency (%)	Yield Strength (MPa)	Elongation (%)
200	112.34	45.85	72.18	1.86
400	156.73	63.97	98.45	2.53
600	184.42	75.27	121.32	3.42
800	162.85	66.47	105.74	2.18
1000	128.67	52.52	83.92	1.75

The optimal tensile properties were achieved at 600 rpm, with a tensile strength of 184.42 MPa, yielding a joint efficiency of 75.27%. This optimal performance can be attributed to the balanced combination of adequate heat input for proper material mixing and controlled intermetallic layer formation (1.58 μm). At this rotational speed, the fracture occurred at the interface between the thermo-mechanically affected zone (TMAZ) and stir zone (SZ) on the aluminium side, rather than at the Al-Fe interface, indicating strong interfacial bonding. At higher rotational speeds of 800 rpm and 1000 rpm, the tensile strength decreased to 162.85 MPa (joint efficiency of 66.47%) and 128.67 MPa (joint efficiency of 52.52%), respectively. This degradation in mechanical properties can be attributed to excessive heat input, resulting in thicker intermetallics layers (1.82 μm and 2.09 μm, respectively) and the formation of defects such as voids and cracks [26]. This behavior can be explained by considering the dual role of the intermetallics layer in determining joint strength.

3.3 Fractography

SEM analysis of the tensile fracture surfaces provided valuable insights into the failure mechanisms of the FSW joints as a function of rotational speed. Figure 9 shows the representative fractographs of joints produced at different rotational speeds. At 200 rpm (Figure 9a), the fracture surface exhibited a mixed-mode character with predominantly interfacial failure along the Al-Fe bond line. As the rotational speed increased to 400 rpm (Figure 9b), the fracture surface showed a higher proportion of dimpled regions, suggesting improved bonding and more extensive plastic deformation before failure. However, the presence of flat regions and occasional cleavage facets indicated that interfacial failure remained a significant fracture mechanism.

At 600 rpm (Figure 9c), the fracture surface exhibited predominantly ductile characteristics, the fracture occurred at the TMAZ/SZ interface on the aluminium side rather than at the Al-Fe interface, indicating that the interfacial bond strength exceeded the local strength of the aluminium alloy in its softened condition. At higher rotational speeds of 800 rpm and 1000 rpm (Figure 9d and 9e), the fracture surfaces showed increasing evidence of brittle fracture along the intermetallic layer, with characteristic cleavage facets and river patterns.

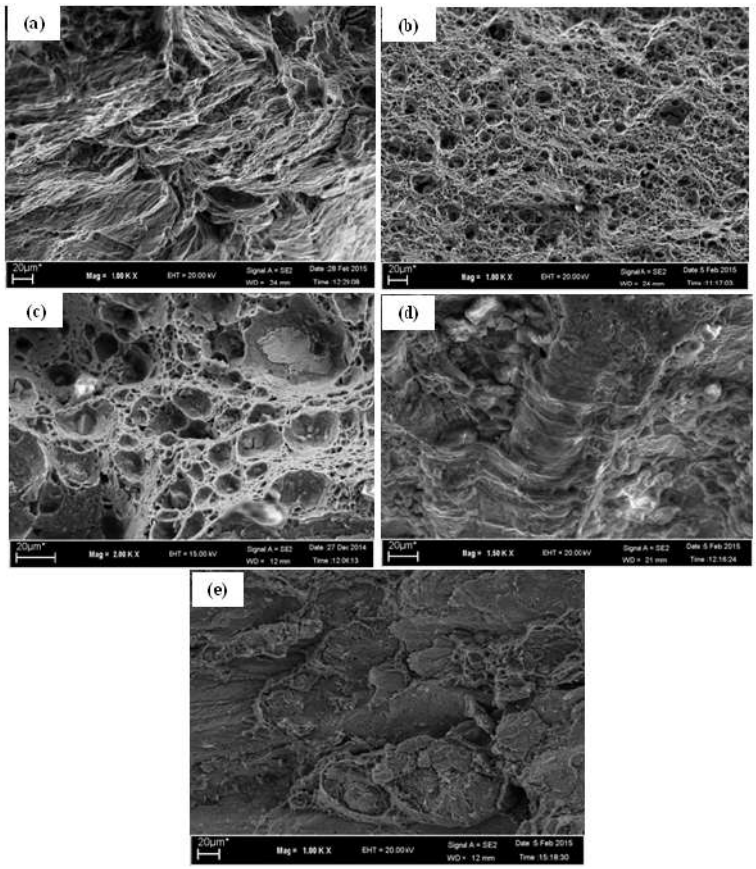

Figure 9 SEM Fractography images at (a) 200 rpm, (b) 400 rpm, (c) 600 rpm, (d) 800 rpm, (e) 1000 rpm.

4. Conclusions

This study investigated the impact of tool rotational speed on friction stir welding (FSW) of AA6351-T6 aluminium and interstitial-free steel, revealing that defect-free joints with optimal mechanical properties were achieved at 600 rpm and 55 mm/min traverse speed. The research demonstrated that aluminium underwent dynamic recrystallization and grain refinement at 400-600 rpm before experiencing grain growth at higher speeds, while steel exhibited continuous grain refinement from 8.7 μm at 200 rpm to 2.6 μm at 1000 rpm. Al-Fe intermetallic layer thickness increased proportionally with rotational speed from 0.87 μm to 2.09 μm, with higher speeds producing uniform but cracked layers that significantly influenced joint performance. The tensile strength peaked at 600 rpm achieving 184.42 MPa with 75.27% joint efficiency, corresponding to an optimal intermetallic thickness of approximately 1.6 μm.

5. CONFLICT OF INTEREST

The authors declare that they have no known competing financial interests or personal relationships that could have appeared to influence the work reported in this paper. This work was completed without any external funding support.

6. Acknowledgements

The authors gratefully acknowledge the institutional support provided by the National Institute of Technology, Patna, for the technical and research work.

7. References

[1] Li WY, Li J, Zhang Z, Gao DL, Wang W, Dong C. Dissimilar metals joining by friction stir welding and friction stir spot welding: A review. J Mater Res Technol. 2024;28:5848-5879.

[2] Mehta KP, Badheka VJ. A review on dissimilar friction stir welding of copper to aluminium: Process, properties, and variants. Mater Manuf Process. 2022;37(5):533-573.

[3] Goyal A, Garg RK. Advances in friction stir welding of dissimilar aluminium alloys: A review. J Mater Res Technol. 2023;23:2882-2909.

[4] Wang H, Wang H. A review on the development of friction stir welding technology for joining aluminium alloys to steel. J Adv Join Process. 2024;9:100172.

[5] Yong E, Chen G, Xie Y, Huang Y, Gao Y. Microstructural evolution and mechanical properties of friction stir welded dissimilar 6061 aluminium alloy/TRIP steel joints. Mater Today Commun. 2023;35:106085.

[6] Saravanan V, Rajakumar S, Banerjee N, Amuthakkannan R. Effect of shoulder diameter to pin diameter (D/d) ratio on microstructure and mechanical properties of dissimilar friction stir welded AA6351-T6 and AISI 304 joints. Arch Civ Mech Eng. 2022;22(3):140-152.

[7] Kang M, Kim C. Joining Al 5052-H32 alloy to steel by friction stir welding: Influence of tool design and process parameters on lap joint properties. J Mater Process Technol. 2022;309:117708.

[8] Kasai H, Morisada Y, Fujii H. Behavior of intermetallic compound formation in dissimilar friction stir welding of aluminium alloy and steel. Mater Sci Eng A. 2023;855:144009.

[9] Shirazi H, Kheirandish S, Safarkhanian MA. Effect of pin offset on the microstructure and mechanical properties of friction stir welded aluminium/steel joints. J Manuf Process. 2022;83:173-185.

[10] Sahu S, Bhat S, Lakshminarayanan AK. Artificial intelligence assisted optimization of friction stir welding parameters for dissimilar aluminium-steel joints. J Manuf Process. 2024;107:412-425.
[11] Thomas WM, Nicholas ED, Needham JC, Murch MG, Temple-Smith P, Dawes CJ. Friction stir butt welding. International Patent Application No. PCT/GB92/02203; 1991.
[12] Eslami N, Haddadi F, Cater S. Intermetallic formation in aluminium to steel friction stir welds: A comprehensive review. Mater Sci Eng A. 2023;863:144523.
[13] Ramachandran KK, Murugan N. Tool trajectory and its effects on dissimilar aluminium-steel friction stir welding. J Mater Eng Perform. 2023;32:8019-8034.
[14] Kumar S, Wu CS. Heat transfer and material flow characteristics in friction stir welding of dissimilar Al-Fe joints. Sci Technol Weld Join. 2022;27(6):488-499.
[15] Khodaverdizadeh H, Mahmoudi A, Heidarzadeh A, Nazari E. Correlation between process parameters and Fe-Al intermetallic compounds in friction stir welded AA6061-T6 aluminium alloy to AISI 304 stainless steel. Mater Chem Phys. 2023;295:127052.
[16] Liu X, Lan S, Ni J. Progress in dissimilar friction stir welding of aluminium alloy and steel: A review. Mater Des. 2023;225:111483.
[17] Abbasi M, Givi MKB, Backgrounds IJ. Fracture mechanisms in dissimilar Al/Fe friction stir welds: Effects of intermetallic compound thickness and welding parameters. Eng Fract Mech. 2022;273:108718.
[18] Tongne A, Desrayaud C, Jahazi M, Feulvarch E. On material flow in friction stir welded Al alloys. J Mater Process Technol. 2023;313:117926.
[19] Wang K, Shen J, Ren Y, Sun Q. Effect of tool pin diameter on microstructure and mechanical properties in friction stir welding of dissimilar Al/Fe joints. Mater Charact. 2024;207:113341.
[20] Shen Z, Ding Y, Chen J, Gerlich AP, Amirkhiz BS. Direct bonding of aluminium to steel by friction stir welding: Interfacial microstructure and mechanical behavior. Mater Sci Eng A. 2023;868:144866.
[21] Frigaad O, Grong O, Middling OT. J Metall Mater Trans A. 2001;32(5):1189-1200.
[22] Kumar S, Wu CS. Heat transfer and material flow characteristics in friction stir welding of dissimilar Al-Fe joints. Sci Technol Weld Join. 2022;27(6):488-499.
[23] Kasai H, Morisada Y, Fujii H. Behavior of intermetallic compound formation in dissimilar friction stir welding of aluminium alloy and steel. Mater Sci Eng A. 2023;855:144009.
[24] Eslami N, Haddadi F, Cater S. Intermetallic formation in aluminium to steel friction stir welds: A comprehensive review. Mater Sci Eng A. 2023;863:144523.
[25] Khodaverdizadeh H, Mahmoudi A, Heidarzadeh A, Nazari E. Correlation between process parameters and Fe-Al intermetallic compounds in friction stir welded AA6061-T6 aluminium alloy to AISI 304 stainless steel. Mater Chem Phys. 2023;295:127052.
[26] Chen K, Liu X, Ni J. Mechanism of intermetallic compound formation at the interface of friction stir welded aluminium/steel joints: A computational and experimental study. Mater Des. 2023;227:111692.